
Article:
Bamiduro, F orcid.org/0000-0002-1914-5731, Guozhao, J, Brown, AP orcid.org/0000-0001-9692-2154 et al. (3 more authors) (2017) Spray-Dried Sodium Zirconate: A Rapid Absorption Powder for CO2 Capture with Enhanced Cyclic Stability. ChemSusChem, 10 (9). pp. 2059-2067. ISSN 1864-5631

https://doi.org/10.1002/cssc.201700046

Spray Dried Sodium Zirconate: A Rapid Absorption Powder for CO_2 Capture with Superior Cyclic Stability

Faith Bamiduro[a], Guozhao Ji[b], Andy P. Brown[a], Valerie A. Dupont[a], Ming Zhao*[b], and Steve J. Milne*[a]

Abstract: Improved powders for capturing CO_2 at high temperatures are required for H_2 production using sorption enhanced steam reforming. This paper examines the relationship between particle structure and carbonation rate for two types of Na_2ZrO_3 powder. Hollow spray-dried micro-granules with a wall thickness of 100-300 nm corresponding to the dimensions of the primary acetate derived particles gave ~75 wt.% theoretical CO_2 conversion after a process-relevant 5 min exposure to 15 vol.% CO_2. A conventional powder prepared by solid state reaction carbonated more slowly, only achieving 50 % conversion due to a greater proportion of the reaction requiring bulk diffusion through the densely agglomerated particles. The hollow granular structure of the spray dried powder was retained post-carbonation but chemical segregation resulted in islands of an amorphous Na-rich phase (Na_2CO_3) within a crystalline ZrO_2 particle matrix. Despite this phase separation, the reverse reaction to re-form Na_2ZrO_3 could be achieved by heating each powder to 900 ℃ in N_2 (no dwell time). This resulted in a very stable multicycle performance in 40 cycle tests using thermogravimetric analysis for both powders. Kinetic analysis of thermogravimetric data showed the carbonation process fits an Avrami-Erofeyev 2-D nucleation and nuclei growth model, consistent with microstructural evidence of a surface driven transformation. Thus, we demonstrate that spray-drying is a viable processing route to enhance the carbon capture performance of Na_2ZrO_3 powder.

Introduction

Powder sorbents for CO_2 at high temperatures are of interest for a number of applications, including the production of H_2 by steam reforming, whereby removal of CO_2 shifts the chemical equilibrium in favour of greater H_2 yield and purity. Sorption enhanced steam reforming, SESR, based on a CaO sorbent ($CaO_{(s)} + CO_{2(g)} \leftrightarrows CaCO_{3(s)}$) has been demonstrated at the research level.[1] Calcium oxide sorbents work best at ~600-700 ºC, and hence couple to the steam reforming reactions; the sorbent may be regenerated by calcination in air at ~800 ºC or above. This type of calcium looping technology has been considered widely for post-combustion capture (PCC) from fossil fuel fired power plants (notably coal-fired) and other single-point industrial emitters.[2] The technology could be implemented using two parallel, fluidized beds operating as carbonator and regenerator, or using fixed bed reactors with alternating carbonation-calcination reactions via feed flow control.[2] For proposed implementation in post combustion capture, the de-carbonation step would be carried out in a near pure CO_2 stream, necessitating calcination temperatures ≥ 950 ºC.[2] In sorption enhanced steam reforming applications where oxygen looping is employed to exchange oxygen with the metal catalyst, air (oxygen depleted) would be the sorbent regeneration stream at temperatures ≥ 800 °C.[1]

An acceptable sorbent for PCC or SESR should have a high CO_2 uptake capacity per unit mass and retain close to its original CO_2 capture capacity over repeated carbonation/regeneration cycles.[3] Material costs should be low, and the sorbent should be mechanically robust, as in the case of calcium oxide and other inorganic oxides. Calcium oxide from limestone is the cheapest and most readily available option. CaO however shows serious loss of CO_2 capacity after repeated calcination cycles at 800 ℃ due to the effects of partial sint ering and loss of surface area and porosity.[4]

A number of additive powders (e.g. SiO_2, Al_2O_3, ZrO_2) have been investigated as means of improving the multi-cycle stability of CO_2 capture performance of the active CaO component.[3] The greater the volume fraction of refractory additive the more durable the sorbent, but there is a trade-off in that dilution of the active component leads to loss of initial capture capacity: 20-30 wt.% is a common compromise loading. The added oxide component often reacts with CaO to form a binary compound, and it is this compound e.g. $Ca_{12}Al_{14}O_{33}$ (mayenite) which acts as the 'refractory spacer' second phase designed to inhibit CaO particle sintering and densification.[3g-k] A uniform distribution of the second phase is essential in order to minimise densification of the active CaO phase and supress multi-cycle degradation. The performance of a range of CaO-based sorbents is summarised in the study of Zhao et al.[3m] The more complex (and costly) the processing technique, e.g. sol-gel or chemical templating, the finer the particle size, and the more uniform the dispersion. Consequently, solution-derived composite powders generally have the best multi-cycle performance relative to the base CaO sorbent material.

Another approach to avoiding multi-cycle powder densification problems has been to use alternative sorbent materials to CaO, such as Li_4SiO_4 and Li_2ZrO_3.[5] The latter has received considerable attention for both post- and pre-combustion capture, and for SESR applications. It absorbs CO_2 according to the reversible reaction: $Li_2ZrO_3(s) + CO_2(g) \leftrightarrows Li_2CO_3(s) + ZrO_2(s)$ (giving a maximum increase in sorbent mass of 28%). It also acts as a basic catalyst which has the advantage of promoting tar degradation in SESR processes. However, its utilisation has been inhibited by poor reaction kinetics at low CO_2 partial pressures (<0.2 bar) and high temperatures (>500 ºC). The more active metastable tetragonal crystal structure, the major contributor to CO_2 chemisorption, is potentially transformed to a less reactive monoclinic form during high temperature cycling. The Li_2ZrO_3 based sorbents are best suited

[a] Drs. F. Bamiduro, A.P. Brown, V.A. Dupont and S.J. Milne
School of Chemical and Process Engineering, University of Leeds, Leeds LS2 9JT, United Kingdom.
E-mail: s.j.milne@leeds.ac.uk (SJM)
[b] Drs. G. Ji and M. Zhao
School of Environment, Tsinghua University, Beijing 100084, China.
E-mail: ming.zhao@tsinghua.edu.cn (MZ)

Supporting information for this article is given via a link at the end of the document.

to processes operating at temperatures <550 °C such as steam reforming of simple compounds such as methane, ethanol or glycerol. Solid solutions of Li_2ZrO_3 with Na_2ZrO_3 have also received attention.[6]

There are also reports of the use of Na_2ZrO_3 and K_2ZrO_3 as CO_2 sorbents.[7] From thermodynamic considerations, Na_2ZrO_3 and K_2ZrO_3 absorb CO_2 at lower CO_2 partial pressures and higher temperatures than Li_2ZrO_3. However K_2ZrO_3 sorbents are more difficult to regenerate. To reach a good balance between ease of capture and regeneration at high temperatures (~650-750 ℃), Na_2ZrO_3 is more promising than either Li_2ZrO_3 or K_2ZrO_3.

The CO_2 uptake and regeneration of Na_2ZrO_3 proceed according to the reversible reaction: $Na_2ZrO_3(s) + CO_2(g) \leftrightarrows Na_2CO_3(s) + ZrO_2(s)$. Conventionally, Na_2ZrO_3 sorbents are synthesised via solid-state reaction between Na_2CO_3 and ZrO_2 at high temperatures (≥1000 °C), resulting in large (micrometre) agglomerated particles, with long diffusion paths for subsequent carbonation.

In order to reduce the particle size of Na_2ZrO_3 sorbents, a number of solution-based synthesis routes have been developed.[7a, 8] These result in faster carbonation rates since a greater proportion of the CO_2 uptake occurs via interfacial solid-gas reactions, and the diffusion lengths for ion migration in the later stages of the reaction (where the rate of mass transfer is controlled by solid state diffusion) are reduced.

In the present paper, we use scanning and transmission electron microscopy with energy dispersive analysis of X-rays (EDX) to investigate the microstructural differences between Na_2ZrO_3 particles produced by spray drying a mixed acetate solution, and powders prepared by conventional solid state reaction. The structural differences we identify account for much faster rates of carbonation in spray dried forms. A CO_2 conversion of ~0.18 g-CO_2 g-sorbent^{-1} (~75% of theoretical capacity) is demonstrated for the spray dried powder after only 5 min exposure to 15 vol.% CO_2 at 700 ℃, viz. under carbonation conditions pertinent to SESR. Stable multi-cycle performance is demonstrated for both powder types over a 40 cycle thermogravimetric testing program (decarbonation at 900 ℃) but due to the slower rate of carbonation for the conventionally prepared Na_2ZrO_3, its conversion is only ~50% of theoretical capacity under these conditions (which are relevant to implementation in SESR). Finally, we link our microstructural observations to kinetic modelling of the CO_2 absorption profiles measured during carbonation in order to gain mechanistic insight into the surface driven absorption process.

Results and Discussion

Phase Analysis and Particle Structure: as-prepared powders

X-ray diffraction patterns confirmed that both spray dried (SD) and solid state (SS) powders contained crystalline Na_2ZrO_3, in the form of hexagonal and monoclinic polymorphs. Figure 1 presents the XRD pattern for the SD powder. Minor peaks ZrO_2 (monoclinic) and very weak peaks of Na_2CO_3 were detected, consistent with residual intermediate phases from the following reaction (Eqn. R1, only inorganic products are represented):

$$2Na(CH_3COO) + Zr(CH_3COO)_4 \rightarrow Na_2CO_3 + ZrO_2 \rightarrow Na_2ZrO_3 + CO_2 \quad (R1)$$

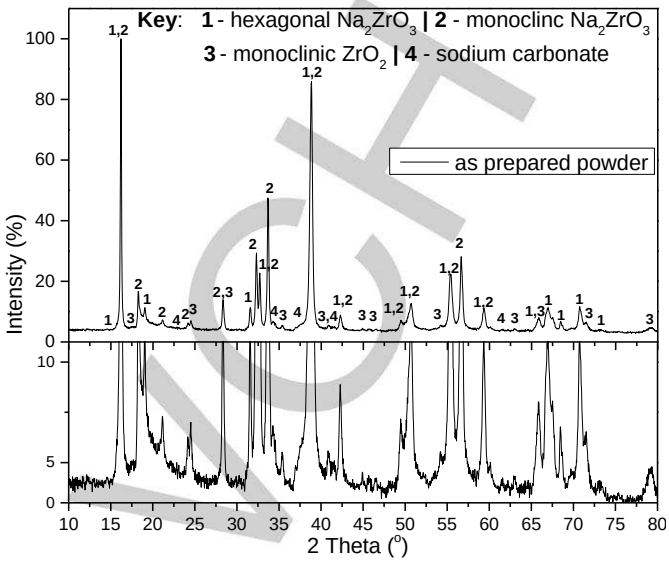

Figure 1. XRD pattern for the Na_2ZrO_3 spray dried powder (top figure) with indexing to a mixture of the hexagonal and monoclinic phases. An expanded intensity scale in the lower figure aids the identification of small quantities of residual intermediate Na_2CO_3 and ZrO_2 phase.

The very weak Na_2CO_3 peaks relative to the XRD peaks for ZrO_2 are consistent with the former being poorly crystallised. The conventional solid state (SS) powder gave similar diffraction patterns to the spray dried material (Figure S1 in the Supporting Information).

Scanning electron microscopy, Figure 2, revealed the SD powders to be hollow, perforated and partially collapsed spherical granules. These ranged in size from ~1-10 µm, Figure 2a. The walls of the granules were composed of interlocking primary particles, 100-300 nm in size, Figure 2b and were a single-(primary) particle in thickness (the 100-300 nm wall thickness is illustrated in Figure S2, Supporting Information). We have observed similar particle structures previously, for example in ZrO_2 granules spray dried from acetate solution.[9] This type of structure is consistent with a formation mechanism in which liquid 'atomised' droplets on entering the heated chamber of the spray dryer first develop a solid, pliable surface skin of salt particles which surrounds a liquid core. On continued heating, pressure builds up and is released by bursting of the outer solid skin, resulting in characteristic surface rupturing of the hollow granule. If the outer skin remains pliable at this stage, the walls collapse to create deformed, hollow spheres. The expelled liquid from the interior of the droplet forms a secondary aerosol which results in a series of smaller granules. A schematic of the proposed SD granule formation mechanism is shown in Figure 3.

The SS powders were composed of densely agglomerated granules, 10s of µm in size, typical of a conventionally prepared mixed oxide ceramic powder; primary particle size was ~ 0.05-1 µm, Figure 2c and 2d.

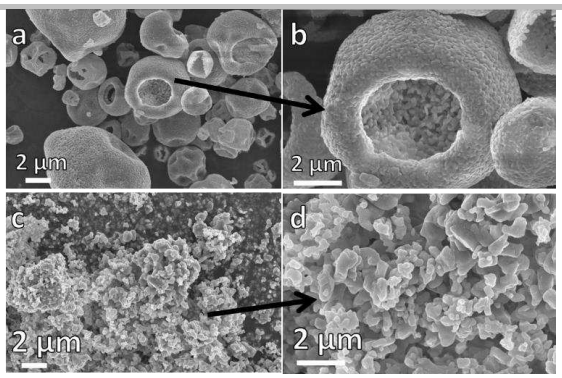

Figure 2. (a and b) SEM images of the spray-dried sorbent powders showing partially deflated, hollow granules 1-10 µm in size with a substructure composed of 100-300 nm primary particles; (c and d) conventional powder prepared by solid state reaction with solid agglomerates 10s µm in size and primary particle size ~1 µm.

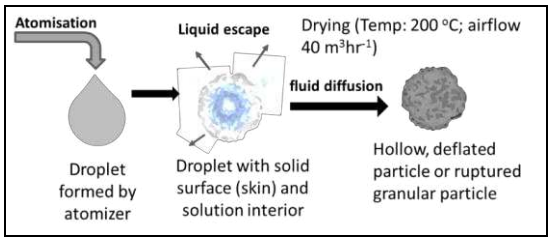

Figure 3. Schematic of Na_2ZrO_3 particle formation during spray drying showing the likely formation route of hollow, ruptured granules; the released liquid goes on to form smaller secondary granules.

Carbonation Characteristics and Effect on Particle Structure

In order to assess the baseline CO_2 uptake performance of the SD and SS powders, the response to prolonged exposure to 15 % CO_2 at 700 ℃ was analysed, Figure 4. The SD powders reached a steady-state increase in mass after ~10 min, equivalent to 0.20 g-CO_2 g-sorbent^{-1} uptake and a molar conversion of ~85% of theoretical capacity. After 5 min the uptake was ~0.18 g-CO_2 g-sorbent^{-1}. The SS powder approached a similar steady state level of carbonation but required a dwell period of almost 25 min as opposed to only 10 min for the SD powder, indicating a much slower rate of carbonation in the conventional SS powder.

The XRD patterns of both powders collected after the end of the isothermal TGA experiment were similar. The pattern for the SD powder is shown in Figure 5, indicating a mixture of Na_2CO_3 and ZrO_2, with no evidence of unreacted Na_2ZrO_3, Figure 5. (The carbonated SS powder pattern appears in the Supporting Information). This confirms the carbonation reaction of the Na_2ZrO_3 phase contained in the calcined starting powder (Eqn. R2) had reached completion (subject to XRD detection limits).

$$Na_2ZrO_3 + CO_2 \rightarrow Na_2CO_3 + ZrO_2 \qquad (R2)$$

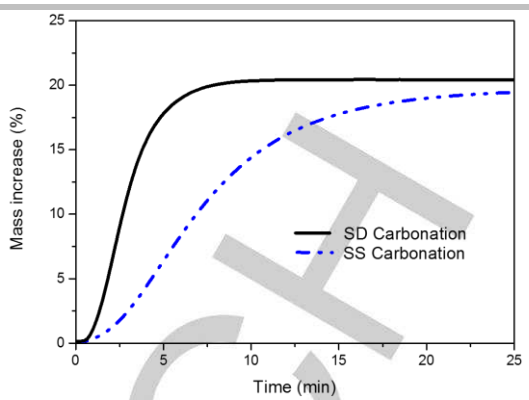

Figure 4. TGA profiles of SD and SS powders carbonated under isothermal conditions (700 ℃, 15 % CO_2).

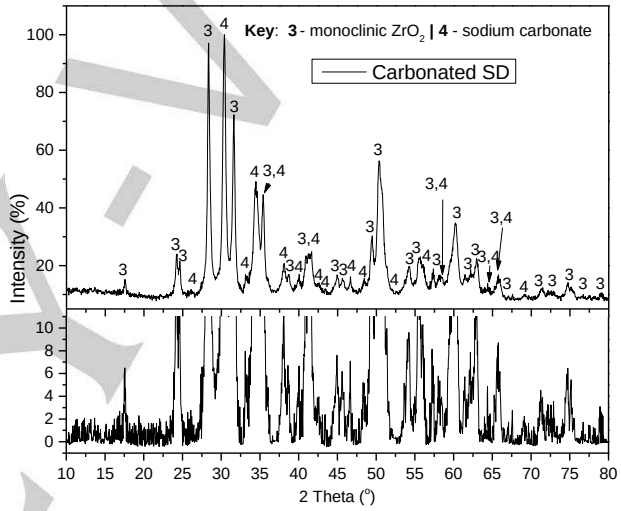

Figure 5. XRD pattern of granules obtained after extended carbonation of the spray dried sorbent (25 min carbonation) revealing the presence of a mixture of ZrO_2 and Na_2CO_3 carbonation products with no other phases detected.

The SEM micrographs of the powders produced after 25 min isothermal carbonation revealed the carbonated SD granules retained the general structure of the as-prepared material Figure 6a (compared to Figure 2b); likewise there was little change in the general form of the SS agglomerates, Figure 6c (compared to Figure 2c). The surface of the carbonated SD granules revealed localised pockets with a smooth, glass-like appearance.

Figure 6a. Close inspection indicated a similar phase was also interspersed within the interlocking sub-micron particles which made up the remainder of the granule surface. The SEM-EDX elemental maps indicated the smooth regions to be Na-rich (Figure 6b), and therefore we attribute these to be sodium carbonate, which under the carbonation conditions employed had softened and flowed into isolated islands. The remainder of the carbonated granule structure was made up of interlocking faceted particles which were Zr-rich (Figure 6b) - these are assumed to be the ZrO_2 phase identified by XRD. There was also some localized glass-like phase interspersed within the (crystalline) ZrO_2 particles. The SS agglomerates showed similar evidence of a glass-like Na-rich phase surrounding Zr-rich particulate material (Figure 6d).

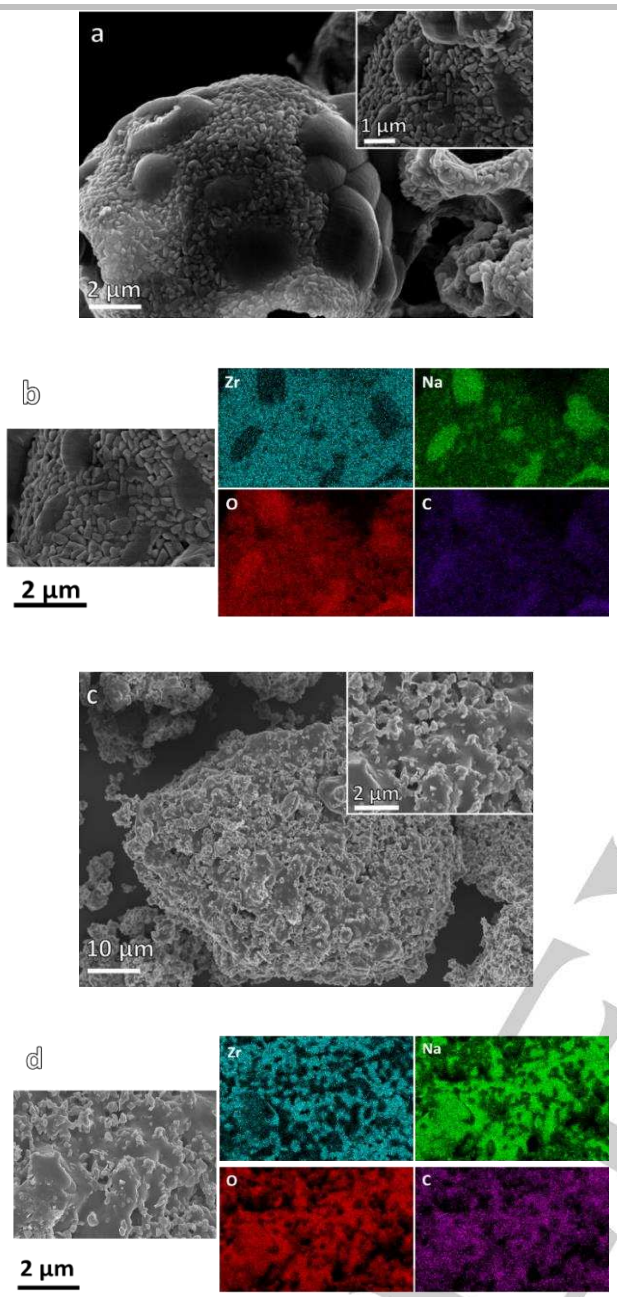

Figure 6. (a) SEM micrograph of spray dried, SD, granules obtained after extended carbonation (25 min 15% CO_2 at 700 °C); (b) EDX mapping of the surface of the SD granule; (c) conventional solid state, SS, powder after carbonation; (d) EDX mapping of the surface of the SS agglomerate.

Multi-cycle Carbonation–Decarbonation Performance

The multi-cycle performance of the spray dried powder and the conventional powder over 40 TGA carbonation-decarbonation cycles, is summarised in Figures 7 (multicycle TGA plots are shown in the Supplementary Information). An increase in the level of CO_2 uptake was observed over the first 3 cycles for each powder; this type of self-activation has been observed for other oxide sorbent powders e.g. CaO and can be attributed to the generation of porosity in the powder due to outgassing in the first few decarbonation cycles.[10] After the initial self-activation period the uptake capacity of both the SD and SS powders showed a remarkable stability, indicating high durability to be an intrinsic feature of sodium zirconate sorbents (as discussed below). The variation in mass conversion of the SD powder was <5 % between cycles number 3 and 40. The CO_2 uptake level was ~0.18 g-CO_2 g-sorbent^{-1} (4.1 mmol g^{-1}) in Cycle 4 corresponding to a molar conversion efficiency of ~75%. Because of the slower rate of carbonation of the SS powder (as identified in Figure 4) the level of uptake after the set 5 min carbonation within multi-cycle experiments was lower, 0.12 g-CO_2 g-sorbent^{-1} (2.7 mmol g^{-1}) or ~50 % conversion by mass under multicycle conditions.

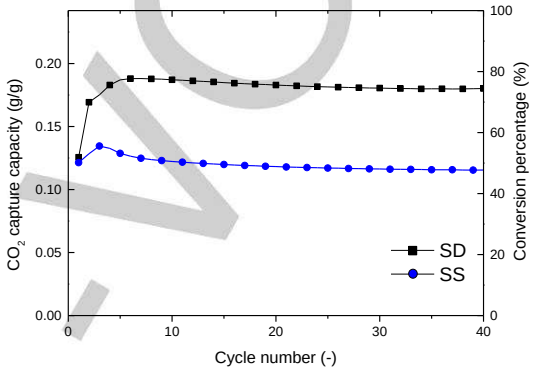

Figure 7. Carbonation performance for spray dried SD and conventional solid state powders SS (carbonation 5 min in 15% CO_2 at 700 °C, regeneration by increasing temperature to 900 °C at 20 ℃ min^{-1} in N_2).

Scanning electron micrographs showed the particle structure of de-carbonated SD and SS powders after 10 and 30 TGA cycles indicated a more porous structure, Figure 8a and 8b, than for the as-prepared example (Figure 2). This is consistent with reports for other oxide sorbents for which an initial increase in porosity due to self-activation associated with the first few carbonation-decarbonation cycles is shown.[10-11] The cycled SS powders were also more porous than the as-prepared SS samples, Figure 8c and 8d.

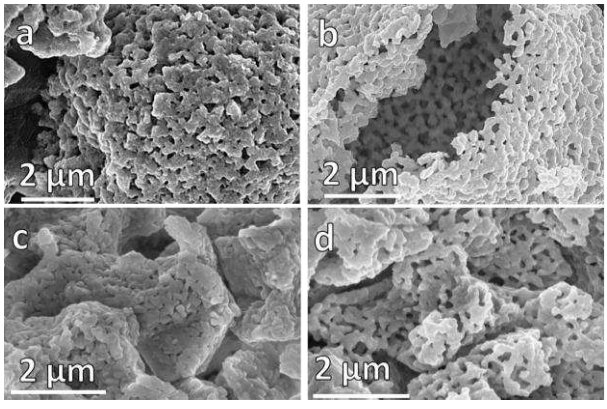

Figure 8. SEM images showing the morphology and surface structure of spray dried SD granules after multi-cycle TGA ending on carbonation: a) 10 cycles

and b) 30 cycles. Corresponding images of the SS powders are shown in c) and d).

Transmission Electron Microscopy of Spray Dried Powder

Analysis by TEM of the carbonated spray dried powder after one TGA cycle and dispersion in heptane is shown in Figure 9a. Only fragments of the granules could be imaged as full size granules were not electron transparent. The fragment has a polycrystalline substructure (top right image in Fig 9a). Lattice imaging of this region reveals crystalline particles in a glassy matrix (bottom right image) with fast Fourier Transform (inset) showing the lattice spacing of the particle identified in the red box to be 2.89 nm, consistent with the ZrO_2 (111) spacing [ICDD ref file 00-037-1484]). EDX spectra (bottom left, Fig 9a) show the polycrystalline regions (red) are Zr and O rich while EDX spectra of the glassy regions (black) are Na and C rich consistent with Na_2CO_3 (the background Cu signal is from the support grid). These findings are in agreement with the information inferred by SEM-EDX of full-size SD granules imaged following extended carbonation experiments (Figure 6) and confirm the walls of the hollow granules are composed of a network of interlocking sub-micrometre, crystalline ZrO_2 particles with regions of partially glassy Na_2CO_3 phase interspersed between them (only partially glassy because XRD identifies a minor amount of crystalline Na_2CO_3).

In order to reveal more information on the spatial distribution of the component phases, two other TEM samples were prepared - a sample collected after 1 TGA cycle, the other after 20 cycles. This time powders were dispersed in acetone instead of heptane. Acetone is a polar solvent in which sodium carbonate and any hydroxyl-carbonate phases that may form on storage in air, or on exposure to moisture present in dispersant liquids (e.g. bicarbonate), are soluble and leach out of the granule fragments. TEM showed that the acetone-dried samples were indeed more porous (Figure 9b) suggesting that soluble (Na_2CO_3) material had originally been located between the ZrO_2 nanoparticle networks, corroborating the interpretations of SEM micrographs (which showed glassy material amongst ZrO_2 particles in addition to segregated pockets of Na_2CO_3). In some areas of the 20 cycle image the leached carbonate phase has re-precipitated in an acicular morphology.

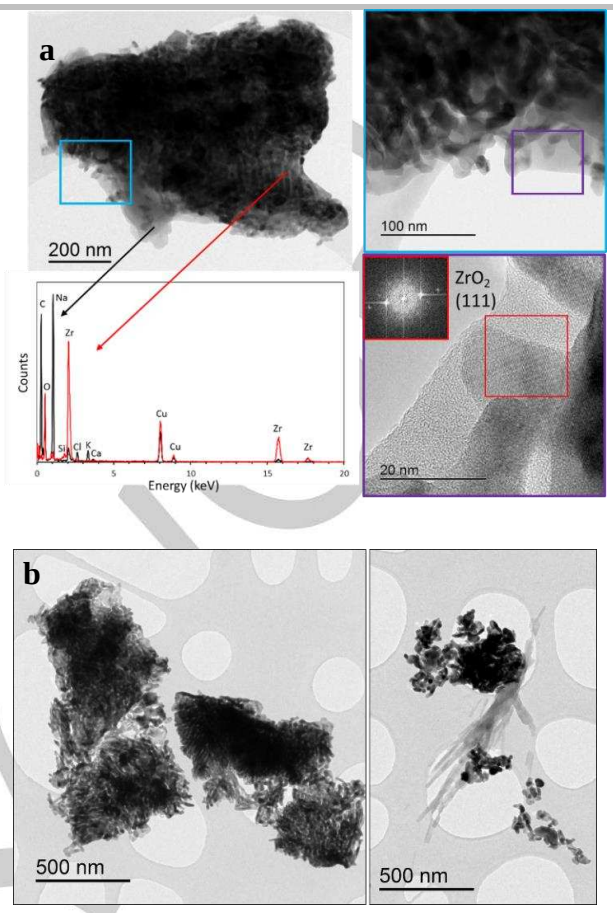

Figure 9. (a) TEM of the carbonated spray dried powder after one TGA cycle and dispersion in heptane. Top left, bright field TEM image of a granule fragment that has a polycrystalline substructure, as highlighted by the high magnification inset (top right, blue box). Lattice imaging of this region is shown in the bottom right image (purple box) and inset shows fast Fourier Transform. EDX spectra (bottom left) of two different regions of the particle: the polycrystalline network regions (red) are Zr and O rich while the glassy region is Na and C rich (the background Cu signal is from the support grid). (b) TEM images of carbonated spray dried granule fragments after 1 TGA cycle (left hand image) and 20 TGA cycles (right hand image) following dispersion in acetone.

Carbonation Reaction: Kinetic Analysis

A set of isothermal TGA carbonation experiments were designed to identify the reaction model that best describes the carbonation process of the SD and SS powders and to derive apparent kinetic parameters.

Conversion was calculated by finding the minimum and maximum measured TGA masses over the cycle step considered (a cycle consisting of carbonation followed by calcination). For carbonation, the minimum mass is the initial mass m_0 at t = 0, whereas the maximum is the final mass m_f at t = t_f.

$$\alpha(t) = \frac{m(t) - m_0}{m_f - m_0} \quad (1)$$

Conversion vs. time data (α vs. t) can then be represented using several models of solid state (gas) reactions. Hancock and Sharp's method[12] assigns a model or a family of models according to the value of m, as defined in Eqn.2:

$$\ln[-\ln(1-\alpha)] = m\ln t + \ln B \quad (2)$$

where B is a constant. i.e., for conversion values (α) typically between 0 and 0.5, plotting $\ln[-\ln(1-\alpha)]$ vs. ln t produces a straight line fit with gradient m.

Figure 10a shows the linear fit for the SD and SS powders carbonating at 700 ℃ with best fit values of m and ln B.

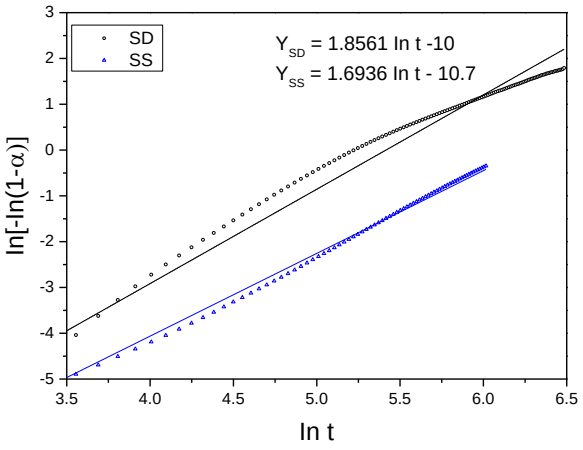

(a)

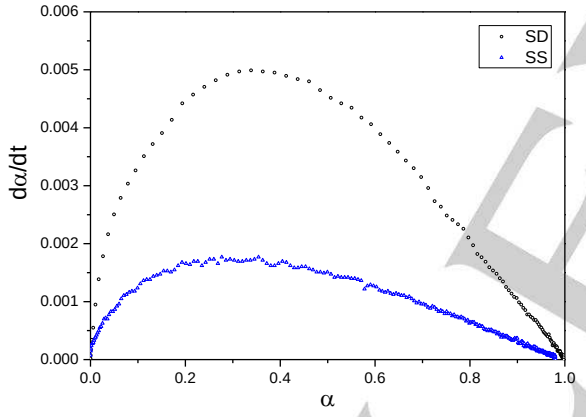

(b)

Figure 10. Model identification for carbonation conversion factors of spray dried (SD) and solid state (SS) powders using (a) Hancock and Sharp method,[12] indicating linear fit with gradient m ~ 2 (Eqn.2) corresponding to Avrami-Erofeyev A2 model; (b) Khawam and Flannagan method [13], indicating dome-shape of dα/dt vs. α

According to Hancock and Sharp [12], the SD and SS powders exhibited m values of 1.86 and 1.69 respectively, both corresponding to Avrami-Erofeyev (also known as 'JMAEK') models close to m = 2, termed 'A2' models. Avrami Erofeyev AN models, with values of N ≥ 1, are known as 'nucleation and nuclei growth models'. In the case of the carbonation of the SD and SS Na_2ZrO_3 crystals, with fitted values of m of 1.9 and 1.7, both closest to N=2 respectively, disc-like are the most likely nuclei shapes.

Further confirmation of the Avrami-Erofeyev model being identified as best fitting the SD and SS Na_2ZrO_3 carbonation reactions is found using the method described by Khawam and Flanagan.[13] In this method, the shape of the plot dα/dt vs. α is used to determine the most likely reaction model, with Avrami-Erofeyev displaying a unique dome-like profile whose apex is located at α values between 0.3 and 0.4 for model 'A2'. Figure 10b shows that the carbonation of both the SD and SS Na_2ZrO_3 powders exhibited dome shapes with apices between 0.3 and 0.4, corresponding roughly to the A2 model.

Reaction kinetics of the Avrami-Erofeyev 'AN' models can be described by the equation relating the 'integral conversion function' g(α) to reaction time following Eqn.3:

$$g(\alpha) = k \times t = (-\ln(1-\alpha))^{1/N} \quad (3)$$

where the rate constant k typically follows Arrhenius' law:

$$k = A \times \exp(-E/RT) \quad (4)$$

Here, the carbonation having been performed at 700 °C, one value of k was obtained for each of the materials tested (SD and SS Na_2ZrO_3 powders).

Inverting Eqns. 1 and 3 allows the calculation of a modelled value of % mass increase as function of time according to Eqns. 5 and 6:

$$\text{model \% mass increase} = 100 \times \frac{m(t) - m_0}{m_0} = \alpha \times \frac{(m_f - m_0)}{m_0} \quad (5)$$

$$\text{With } \alpha = 1 - \exp\left[-\left((kt)^N\right)\right] \quad (6)$$

Figure 11 compares the experimentally obtained % mass increases vs. time of the SD and SS Na_2ZrO_3 powders during carbonation at 700 ℃ with their modelled counterpart using Eqns. 5 and 6, and provides a final test of the suitability of the chosen models with their derived kinetic rates. It can be seen that an excellent match between experimental and modelled mass increases was obtained for both materials.

Both modelling methods indicate 2-D nucleation and nuclei growth for the carbonate phase which when combined with the SEM observations (Figures 2 and 6) suggest a surface driven transformation of the Na_2ZrO_3 granules, consistent with a porous Na_2CO_3 and ZrO_2 surface layer discussed in another Na_2ZrO_3 study.[7d]

In summary, spray dried Na_2ZrO_3 granules exhibit rapid CO_2 uptake reaching 0.18 g-CO_2 g-sorbent^{-1} within only 5 min (15 % CO_2 at 700 ℃) some 50 % greater conversion within this process-relevant time period than the conventionally prepared SS powder. Both powder types are highly durable, showing minimal decay (< 5 %) in uptake capacity after the 40 cycle test under conditions relevant to steam reforming.

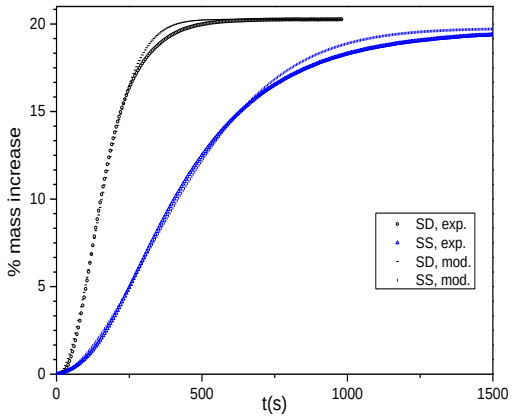

Figure 11. Time profiles of mass increase from experimental TGA compared with modelled mass increases for spray dried (SS) and solid state (SS) powders using Eqns. 5 & 6 with parameters N_{SD} = 1.856, k_{SD} = 5.400 ×10^{-3} s^{-1}, $m_{0,\,SD}$ = 11.07 mg , $m_{f,\,SD}$ = 13.32 mg, N_{SS} = 1.693, k_{SS} = 1.971 ×10^{-3} s^{-1}, $m_{0,\,SS}$= 11

Thus we demonstrate the intrinsically superior durability of sodium zirconate, and demonstrate that the rate of carbonation may be improved through simple spray-drying which is an industrially scalable process that provides a fine primary particle size within a porous granular structure. Confirmation of a higher surface area in the SD powders, as suggested by the SEM micrographs, was obtained from N_2 adsorption isotherms (Figure 12). The BET surface areas of the SD powder were ~20 m^2 g^{-1} compared to only ~ 2 m^2 g^{-1} for the SS powder. Hysteresis in the isotherms indicates mesoporosity. Pore volumes measured via the BJH method were ~ 0.039 cm^3 g^{-1} for the SD powder and 0.007 cm^3 g^{-1} for the SS powder. This difference is consistent with SEM observations of hollow perforated micro-granules in SD powders, and dense agglomerates in SS powders. The hollow and perforated microstructure of the spray dried granules, provides easy access of CO_2 to the inner and outer surfaces of the granule walls. This allied to the thin wall dimensions results in a higher proportion of the carbonation process involving a rapid gas-solid reaction (the linear segment of the TGA profile) than is the case for the densely agglomerated SS Na_2ZrO_3 powder.

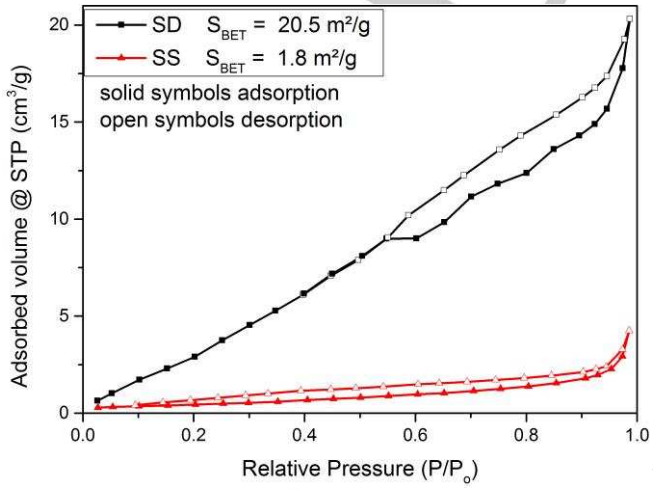

Figure 12. Nitrogen adsorption-desorption isotherms for the Na_2ZrO_3 sorbent powders produced via spray drying (SD) and conventional solid state reaction (SS).

Crystalline sodium zirconate naturally possesses lattice-scale intimate mixing of refractory 'ZrO_2' and active Na_2O' constituents. The crystal structure of the monoclinic form is represented in Figure 13. The lattice-scale distributions of each component represents ideal mixing of a composite metal oxide sorbent material suited to high temperature operation, and account for the remarkable durability of Na_2CO_3 in multicycle operation. This scale of mixing cannot be achieved by mechanical mixing or chemical precipitation of two-phase sorbent and refractory spacer powders.

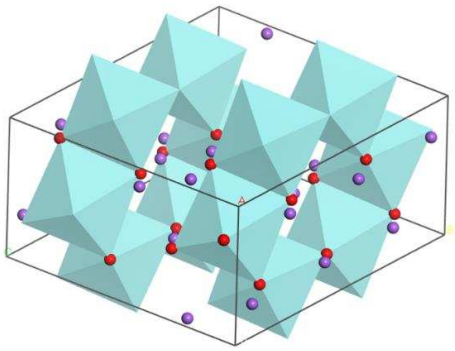

Figure 13. Crystal structure of Na_2ZrO_3 (monoclinic): pale blue polyhedral represent edge-sharing ZrO_6 structural units; red dots are oxygens and purple dots are sodium ions.

During carbonation the Na_2ZrO_3 crystal lattice decomposes in a surface driven process to a truly nanoscale composite of ZrO_2 and Na_2CO_3. From SEM and TEM examination of the walls of the hollow spray dried granules, a poorly crystallised/glassy carbonate phase segregates. The reverse reaction to re-generate crystalline Na_2ZrO_3 occurs readily during the temperature and gas swing decarbonation step, once again creating a sorbent with ideal crystal lattice scale distributions of 'active' and 'spacer' components ready for the next carbonation step. The net result is a very durable single-phase high-temperature sorbent.

As mentioned in the Introduction there is a wide literature on other high temperature powder sorbents for CO_2 capture, most notably for CaO powders in which refractory additives are introduced, for example ZrO_2 [3m, 14] to supress the natural densification (partial sintering) and loss of porosity that degrades cycle on cycle CaO performance, as outlined in the Introduction. Often very complex chemical solution precipitation reactions are employed to promote adequate mixing of the two components. In 2012 we proposed a temperature induced volume-expanding phase change additive to disrupt densification,[15] others later adopted this concept.[16] However we found that the volume expansion that occurred between regeneration and carbonation was accommodated in the residual pore spaces and did not induce micro-cracking to open up porosity prior to the next carbonation step. All of these second-phase additives to a

sorbent powder require complicated processing to achieve significant improvements in durability since performance is only improved if there is intimate mixing of 'refractory' additive and sorbent. Even the best chemical or mechanical synthetic processes only give mixing of the two particle types on the sub-micron scale.

There are a number of literature reports of Na_2ZrO_3 as a sorbent for CO_2: the conditions used for sorption-desorption vary between the different publications. Martínez-dlCruz and Pfeiffer[7d, 7e] prepared Na_2ZrO_3 by a similar solid state route to our SS powder but with calcination at 850 ºC for 6 h and found that addition of 20 % excess Na_2ZrO_3 produced a phase-pure product (by XRD). The surface area of this product was ~ 3 $m^2 g^{-1}$, comparable to the surface area of the SS powder in the present report. Their 20 cycle sorption-desorption studies were conducted in 100 % CO_2 (as opposed to 15 % here): temperatures between 550-700 ℃ were found to give the highest uptakes; desorption, in N_2, was conducted at ≤ 800 °C. Sorption dwell times of 30 minutes were adopted, the samples exhibited CO_2 uptakes corresponding to 18.5-19 mass%[7d, 7e]. Our SS powder exhibited similar uptake after similar total time periods to these reports (Figure 4) but we adopted a shorter, 5 minute, carbonation period in multicycle TGA as this more closely replicated conditions of a working sorbent. The same group studied the microstructure of their solid state powders and concluded that a mesoporous structure was formed on the surface of the agglomerates at sorption temperatures of 300-550 ℃ but sintering of this shell layer at temperatures above 550 ℃ eliminated the porosity and at that stage sorption kinetics were controlled by diffusion processes through a dense Na_2CO_3 + ZrO_2 shell.[7d] This is consistent with our TEM analysis. The effect of relative humidity on the carbonation and decarbonation processes at low temperatures (30-80 ℃) for powders produced by solid state reaction shows that high humidity has a positive effect which was attributed to bicarbonate formation at the surface.[17]

Several solution routes have been used to produce Na_2ZrO_3 sorbent powders. This includes simple evaporation of sodium acetate and zirconium acetyl acetonate in ethanol and uptakes of CO_2 of ~ 21 wt.% by TGA analysis over four cycles were recorded involving sorption in 80%CO_2 at 600 ℃ (for > 100 minutes) and regeneration in argon at 800 ℃. [7a, 8] Spray drying of these precursor solutions was also investigated.[8] Unlike the SD granules of the present work, their spherical granules disintegrated on calcination to produce a nano-sized powder of similar particle sizes, ~ 50 nm, to the powders produced by simple evaporation drying. Hence both spray dried and simple evaporation powders within the study of Zhao et al.[8] exhibited similar CO_2 capture properties; achieving a ~ 17.5 wt.% mass increase after 200 s in 100 % CO_2 at 575 ℃. Multicycle performance in 50 % CO_2 up to 11 cycles indicated an uptake of ~ 15 wt.%.[8] Sodium oxalate and zirconium nitrate, sodium citrate and zirconyl nitrate aqueous solutions as well as sodium acetate and zirconyl chloride solutions have been used to produce Na_2ZrO_3 in an evaporation-drying–calcination process reported by Ji et al.[18] and Zhao et al.[19]]

The CO_2 capture kinetics of our SD powders compare favourably to other Na_2ZrO_3 sorbent powders, although performance comparisons between different laboratories is complicated by the variability in sorption and desorption conditions employed. We demonstrate distinctive microstructural features that lead to high surface areas which explain the reasons for the characteristic rapid rates of carbonation. The direct like-for-like comparison to SS tested under identical TGA conditions provides an unequivocal demonstration of the superior performance of SD. For comparisons with other alkaline metal or alkaline earth ceramic sorbents, the reader is directed to a comprehensive review article by Memon et al.[19]

Conclusions

The microstructural reasons for faster rates of CO_2 capture by spray dried granules of Na_2ZrO_3 relative to a powder prepared by conventional solid state synthesis method have been established using a combination of scanning and transmission electron microscopy, surface area measurements and kinetic modelling. The hollow and perforated granular structure of spray dried powders presents a higher surface area than the densely agglomerated conventional powder and promotes the surface-driven carbonation reaction. This permitted ~75 % of theoretical mass conversion within 5 min exposure to 15 % CO_2 at 700 ℃, compared to only ~50 % for the benchmark conventional solid state powder. Although segregation of Na_2CO_3 and ZrO_2 occurs during carbonation, crystalline Na_2ZrO_3 is reformed by heating to 900 ℃ and immediately cooling, ready for the next carbonation step in a multicycle sorption-desorption process. High multicycle durability is an intrinsic feature of Na_2ZrO_3 as the active soda component is held within a stable crystal structure. This contrasts to alternative high temperature sorbents such as CaO based materials where sintering degrades durability.

Experimental Section

Spray dried powders (SD) were prepared from a starting solution produced by dissolving 50 mmol $Na(CH_3COO)\cdot 3H_2O$) and 25 mmol $Zr(CH_3COO)_2$ in 300 ml dilute nitric acid (Sigma Aldrich reagents) to form a clear solution. This solution was spray dried using a bench-top spray dryer (SD-05 Lab-Plant, UK). The operation conditions were: inlet temperature 200 ºC, aspirating air flow at 40 $m^3 h^{-1}$, peristaltic pump speed 0.6 $dm^3 h^{-1}$ and compressor pressure at 1.8 bar. Collected powders were calcined in a box furnace at 900 ℃ for 2 h to promote formation of Na_2ZrO_3. The conventional solid state powder (SS) was prepared by ball-milling Na_2CO_3 (Acros Organics) and ZrO_2 (Dynamic Ceramics) powders for 16 h, followed by calcination at 900 ℃ for 2 h. Nitrogen adsorption-desorption isotherms were measured using a Quantachrome Instruments Nova 2200: surface areas were measured by the BET method and pore volumes by the BJH method. Samples were outgassed under vacuum at 200 ℃ for 3 h prior to analysis.

The first assessment of the carbonation characteristics of the SD and SS powders involved isothermal thermogravimetric analysis (TGA) in which a ~15 mg sample was exposed to CO_2 at 700 ℃ (Mettler Toledo star 1 TGA/DSC). The sample was first heated to 900 ℃ (20 ℃ min^{-1}) in N_2 to remove any traces of hydrated/carbonated

surface phases formed during storage. After cooling (20 ℃ min^{-1}) to 700 ℃, the gas was switched to 15% CO_2/85% N_2 and held at this condition for 25 min. Multi-cycle performance up to 40 cycles was evaluated using 700 ℃, 15% CO_2/5 min carbonation and regeneration (desorption) achieved by switching to N_2 and heating at 20 ℃ min^{-1} to 900 °C and immediately cooling at 20 ℃ min^{-1} to 700 ℃.

X-ray diffraction (XRD) data were collected using a Bruker D8 diffractometer (Cu-Kα λ=1.5416 Å). Due to the small quantities of powders generated in the TGA experiments, the powders were deposited on a silicon sample holder. The resulting XRD patterns were analysed using X'Pert HighScore Plus software (Version 3.0e). The diffraction patterns were compared to standard patterns in the ICDD PDF4 database (International Centre for Diffraction Data).

The microstructures of as-prepared powders, carbonated powders and powders after multiple carbonation/decarbonation cycles were characterised by using scanning electron microscopy, SEM with energy dispersive X-ray (EDX) elemental analysis (LEO 1530 Gemini field emission gun, FEG-SEM). All samples for SEM were sputter coated with a layer of platinum, ~5 nm in thickness. Transmission electron microscopy was used to analyse a SD sample after 1 and 20 successive TGA cycles, ending on a carbonation step (Philips CM200 Field emission gun TEM/STEM with Supertwin Objective lens, and an Oxford Instruments SD 80 mm^2 X-max EDX system running INCA software). Powders were prepared for TEM by dispersing in either acetone or heptane (as detailed) and drop-casting onto standard holey carbon films supported on copper grids (Agar Scientific Ltd).

Acknowledgements

This work was funded by the Engineering and Physical Sciences Research Council, award number EP/J014702/1. The authors wish to thank Andrew Scott, University of Leeds for generating the structure shown in Figure 13 and to Aidan Westwood for discussions regarding N_2 adsorption data analysis.

Keywords: CO_2 capture • sodium zirconate • spray drying • rapid absorption • kinetic analysis

[1] a) E. J. Anthony, E. M. Bulewicz, L. Jia, Prog. Energy Combust. Sci. **2007**, 33(2), 171-210; b) B. Dou, V. Dupont, P. T. Williams, H. Chen, Y. Ding, Bioresour. Technol. **2009**, 100(9), 2613-2620.

[2] J. C. Abanades, E. J. Anthony, J. Wang, J. E. Oakey, Environ. Sci. Technol. **2005**, 39(8), 2861-2866.

[3] a) V. Manovic, E. J. Anthony, Energ. Fuel. **2010**, 24(10), 5790-5796; b) N. MacDowell, N. Florin, A. Buchard, J. Hallett, A. Galindo, G. Jackson, C. S. Adjiman, C. K. Williams, N. Shah, P. Fennell, Energy. Environ. Sci. **2010**, 3(11), 1645-1669; c) V. Manovic, J.-P. Charland, J. Blamey, P. S. Fennell, D. Y. Lu, E. J. Anthony, Fuel **2009**, 88(10), 1893-1900; dDOE, Carbon Capture and Sequestratio Systems Analysis Guidelines, U.S. Department of Energy, 2005;; eDOE, Hydrogen, Fuel Cells & Infrastructure Technologies Program: Multi-Year Research, Development and Demonstration Plan, 2012, pp. 3.1_1 - 3.1_53; f) A. MacKenzie, D. L. Granatstein, E. J. Anthony, J. C. Abanades, Energ. Fuel. **2007**, 21(2), 920-926; g) Z.-s. Li, N.-s. Cai, Y.-y. Huang, H.-j. Han, Energ. Fuel. **2005**, 19(4), 1447-1452; h) C. S. Martavaltzi, A. A. Lemonidou, Ind. Eng. Chem. Res. **2008**, 47(23), 9537-9543; i) M. Broda, C. R. Müller, Adv. Mater. **2012**, 24(22), 3059-3064; j) R. Koirala, G. K. Reddy, P. G. Smirniotis, Energ. Fuel. **2012**, 26(5), 3103-3109; k) C.-T. Yu, W.-C. Chen, Powder Technol. **2013**, 239, 492-498; l) S. F. Wu, Y. Q. Zhu, Ind. Eng. Chem. Res. **2010**, 49(6), 2701-2706; m) M. Zhao, M. Bilton, A. P. Brown, A. M. Cunliffe, E. Dvininov, V. Dupont, T. P. Comyn, S. J. Milne, Energ. Fuel. **2014**, 28(2), 1275-1283.

[4] a) C. C. Dean, J. Blamey, N. H. Florin, M. J. Al-Jeboori, P. S. Fennell, Chem. Eng. Res. Des. **2011**, 89(6), 836-855; b) X. Wang, M. Li, S. Li, H. Wang, S. Wang, X. Ma, Fuel Process. Technol. **2010**, 91(12), 1812-1818.

[5] a) H. Yang, Z. Xu, M. Fan, R. Gupta, R. B. Slimane, A. E. Bland, I. Wright, Journal of Environmental Sciences **2008**, 20(1), 14-27; b) K. Nakagawa, T. Ohashi, J. Electrochem. Soc. **1998**, 145(4), 1344-1346; c) B. N. Nair, T. Yamaguchi, H. Kawamura, S. I. Nakao, K. Nakagawa, J. Am. Ceram. Soc. **2004**, 87(1), 68-74; d) B. N. Nair, R. P. Burwood, V. J. Goh, K. Nakagawa, T. Yamaguchi, Prog. Mater Sci. **2009**, 54(5), 511-541.

[6] M. Khokhani, R. B. Khomane, B. D. Kulkarni, J. Sol-Gel Sci. Technol. **2012**, 61(2), 316-320.

[7] a) T. Zhao, E. Ochoa-Fernández, M. Rønning, D. Chen, Chem. Mater. **2007**, 19(13), 3294-3301; b) I. Alcérreca-Corte, E. Fregoso-Israel, H. Pfeiffer, J Phys Chem C **2008**, 112(16), 6520-6525; c) G. G. Santillán-Reyes, H. Pfeiffer, Int J Green Gas Con **2011**, 5(6), 1624-1629; d) L. Martínez-dlCruz, H. Pfeiffer, J Phys Chem C **2012**, 116(17), 9675-9680; e) L. Martínez-dlCruz, H. Pfeiffer, J. Solid State Chem. **2013**, 204, 298-304; f) B. Alcántar-Vázquez, Y. Duan, H. Pfeiffer, Ind. Eng. Chem. Res. **2016**, 55(37), 9880-9886.

[8] T. Zhao, M. Rønning, D. Chen, J Energy Chem **2013**, 22(3), 387-393.

[9] a) W. Nimmo, D. Hind, N. J. Ali, E. Hampartsoumian, S. J. Milne, J Mater Sci **2002**, 37(16), 3381-3387; b) W. Nimmo, N. J. Ali, R. M. Brydson, C. Calvert, E. Hampartsoumian, D. Hind, S. J. Milne, J. Am. Ceram. Soc. **2003**, 86(9), 1474-1480; c) G. L. Messing, S.-C. Zhang, G. V. Jayanthi, J. Am. Ceram. Soc. **1993**, 76(11), 2707-2726.

[10] V. Manovic, E. J. Anthony, Environ. Sci. Technol. **2008**, 42(11), 4170-4174.

[11] S. Stendardo, L. K. Andersen, C. Herce, Chem. Eng. J. **2013**, 220, 383-394.

[12] J. D. Hancock, J. H. Sharp, J. Am. Ceram. Soc. **1972**, 55(2), 74-77.

[13] A. Khawam, D. R. Flanagan, The Journal of Physical Chemistry B **2006**, 110(35), 17315-17328.

[14] R. Koirala, K. R. Gunugunuri, S. E. Pratsinis, P. G. Smirniotis, J Phys Chem C **2011**, 115(50), 24804-24812.

[15] V. D. A. P. Brown, S. J. Milne, , New Approach to Extend Durability of Sorbent Powders for Multicycle High Temperature CO_2 Capture in Hydrogen, http://gow.epsrc.ac.uk/NGBOViewGrant.aspx?GrantRef=EP/J014702/1, **2012**.

[16] M. Zhao, J. Shi, X. Zhong, S. Tian, J. Blamey, J. Jiang, P. S. Fennell, Energy. Environ. Sci. **2014**, 7(10), 3291-3295.

[17] J. A. Mendoza-Nieto, H. Pfeiffer, RSC Adv. **2016**, 6(71), 66579-66588.

[18] G. Ji, M. Z. Memon, H. Zhuo, M. Zhao, Chem. Eng. J. **2017**, 313, 646-654.

[19] M. Z. Memon, X. Zhao, V. S. Sikarwar, A. K. Vuppaladadiyam, S. J. Milne, A. P. Brown, J. Li, M. Zhao, Environ. Sci. Technol. **2017**, 51(1), 12-27.

Entry for the Table of Contents

FULL PAPER

The hollow and perforated granular structure of spray dried Na_2ZrO_3 powders enables faster CO_2 absorption than densely agglomerated conventional sorbents.

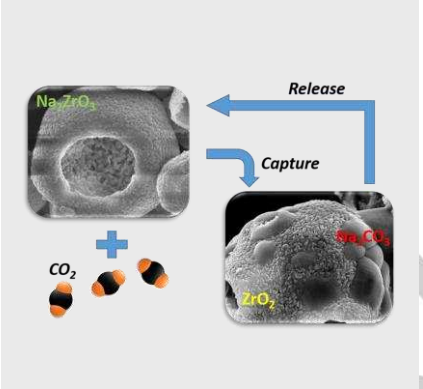

F. Bamiduro, M. Zhao,* A. P. Brown, V. A. Dupont, S. J. Milne*

Page No. – Page No.

Spray Dried Sodium Zirconate: A Rapid Absorption Powder for CO_2 Capture with Superior Cyclic Stability